COMPOSITION AND THERMAL HISTORY OF THE IVB IRON METEORITES. J. Yang[1], J. I. Goldstein[1], J. R. Michael[2], and P. G. Kotula[2], [1]Dept of Mechanical and Industrial Engineering, University of Massachusetts, Amherst, MA 01003, USA. E-mail: jiyang@ecs.umass.edu. [2]Materials Characterization Department, Sandia National Laboratories, PO BOX 5800, MS 0886, Albuquerque, NM 87185, USA.

Introduction: Among the magmatic iron meteorites, group IVB irons have some unusual characteristics, such as high bulk Ni (15-18 wt%), high refractory elements (e.g., Ir), low volatile elements (e.g., Ga, Ge) [1, 2], fast cooling rates and a small parent body [3, 4]. IVB irons do not have a Widmanstatten pattern as in lower Ni IIIAB or IVA irons. Instead, IVB irons have a plessite structure with micron sized kamacite (α) spindles sometimes associated with phosphide (Ph). The microstructure is very different between low Ni and high Ni IVB irons. The low Ni IVB irons have very few kamacite spindles and phosphides while high Ni IVB irons have many more kamacite spindles and significant amounts of phosphides for the same size analysis area. Because of the small micron sized kamacite spindles, the classical metallographic cooling rate methods such as taenite (γ) central Ni vs. half width (Wood) method [5] or taenite (γ) Ni profile matching method [6] have not been applied. Cooling rates for IVB irons have been measured using the kamacite band width method [3, 4, 7]. The measured cooling rates are very fast, >1,000 K/Myr and do not vary with meteorite Ni content [4]. However, the measurement of kamacite band width is not accurate in this study since the orientation of the spindles with respect to the sample surface is unknown and the errors in individual cooling rates vary by a factor about 10 [4]. The cooling rates may not be accurate and the constancy of the measured cooling rates with Ni content may be in doubt [8].

Purpose: In order to understand the IVB thermal history and the nature of its parent body, we have remeasured the IVB cooling rates. We have measured Ni gradients using x-rays generated from thin sections of IVB irons in the electron microscope and have applied the taenite Ni profile matching method [6].

Method: We examined ten IVB irons which were also studied by [2]: Cape of Good Hope, Hoba, Iquique, Santa Clara, Skookum, Tawallah Valley, Tlacotepec, Warburton Range, Weaver Mountains, and Ternera. The samples were first prepared for optical microscopy and observed and analyzed using light optical microscopy and the Cameca SX-50 electron probe microanalyzer (EPMA).

In order to determine the nucleation temperature of the kamacite spindles, it is necessary to have accurate bulk Ni and P contents for each meteorite. Although bulk Ni and P contents have been measured systematically [1, 2], there are significant differences between measured values of the P content. Therefore, our first step was to remeasure the bulk Ni and P content of each meteorite using area scans obtained with the EPMA. The bulk compositions of the major elements Fe, Ni, Co and P were measured in scan areas from 64,000 μm^2 to 216,000 μm^2 for each of the ten IVB irons by EPMA. Since few kamacite spindles and phosphides are present in the low Ni IVBs, the composition is more or less homogeneous and relatively small scan areas can be measured. For high Ni irons, the presence of larger amounts of kamacite and phosphide required larger x-ray scan areas to obtain a representative bulk composition.

The second step was to measure Ni profiles in taenite and adjacent kamacite across kamacite-taenite interfaces as input to the Ni profile matching method. For each IVB iron suitable kamacite spindles and surrounding taenite were thinned for electron microscopy using a dual beam FEI DB-235 focused ion beam (FIB)/SEM instrument at Sandia National Laboratories. We measured the Ni profiles across each kamacite-taenite boundary by x-ray analysis using a FEI Tecnai F30ST field emission transmission - analytical electron microscope (TEM-AEM) at Sandia National Laboratories. The measured Ni profiles are used to match the calculated Ni profiles for various cooling rates from the cooling rate simulation program [9].

Results and Discussion: The bulk Ni and P measured in ten IVB irons are plotted in Fig. 1.

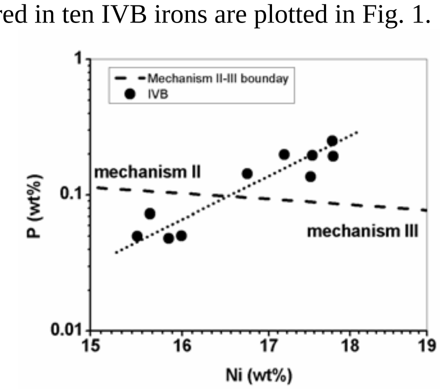

Fig.1. Measured bulk Ni and P in ten IVB irons (trend shown by a dotted line). Also shown are the Ni-P zones in which nucleation mechanism II and III can be applied (separated by a dashed line).

The bulk Ni in ten IVB irons varies from 15.5 to 18 wt% and the bulk P varies from 0.05 to 0.25 wt%. The Ni and P trend is shown by the dotted line in Fig. 1 and developed due to fractional crystallization in the core of the parent asteroid [1, 2]. The measured bulk Ni and P are more or less consistent with the data of Campbell and Humayun [1], but the difference in bulk P is significantly different from that of Walker et al. [2] who measured bulk P values from 0.025 to 0.659 wt%.

The formation of kamacite in iron meteorites is determined by the bulk Ni and P content of the meteorite and by its path through the ternary Fe-Ni P phase diagram as the meteorite cools from the all taenite (γ) field at high temperatures. Depending on the Ni and P content of the meteorite, the kamacite nucleation temperature can be determined from either the $(\gamma + Ph)/(\alpha + \gamma + Ph)$ phase boundary, the $(\alpha + \gamma)/ (\alpha + \gamma + Ph)$ phase boundary, or the martensite start temperature, Ms, where α_2 – martensite forms [10]. The low Ni, low P IVB members cool below the $(\alpha + \gamma)/ (\alpha + \gamma + Ph)$ boundary and kamacite forms by the reaction $\gamma \rightarrow (\alpha + \gamma) \rightarrow \alpha + \gamma + Ph$. The designation $(\alpha + \gamma)$ indicates that the alloy passes through the $\alpha + \gamma$ two-phase field but kamacite nucleation is suppressed. This reaction scheme is called Mechanism III [10]. The high Ni, high P members of IVB pass through the γ + Ph phase field and α-kamacite forms by the reaction $\gamma \rightarrow \gamma + Ph \rightarrow \alpha + \gamma + Ph$, Mechanism II [10]. Figure 1 shows the Ni-P regions where mechanisms II and III are applicable for the nucleation of the kamacite spindles in IVB irons. Irons with bulk Ni and P located above the dashed line nucleate kamacite at high temperatures by mechanism II while irons with bulk Ni and P located below the dashed line nucleate kamacite at low temperatures by mechanism III. Nucleation temperatures for kamacite (spindle) formation can be obtained from the relevant Fe-Ni-P phase diagrams. Rasmussen proposed that P is saturated in taenite before reaching the $(\gamma)/(\alpha + \gamma)$ boundary on the equilibrium phase diagram during the cooling process [3, 4]. This assumption is incorrect for the low P IVB irons and leads to inaccuracies in the cooling rate measurements.

Measured and calculated Ni profiles across kamacite-taenite boundaries for Hoba (low Ni, low P IVB) and Warburton Range (high Ni, high P IVB) are shown in Fig. 2. The x-ray spatial resolution is 4 nm and about 500 measurements can be obtained in a 2 μm gradient (see Fig. 2). We applied the metallographic cooling rate program [9] to calculate the cooling rate for each of the IVB irons. Two examples are shown in Fig. 2. The cooling rate of Hoba is about 700 K/Myr and the cooling rate of Warburton Range is about 3,000 K/Myr. These cooling rates vary by at least a factor of 6 across the IVB group, in contrast to previous measurements [3, 4].

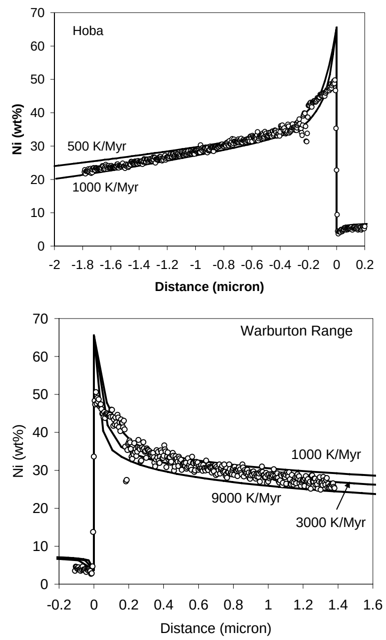

Fig. 2. Measured Ni profiles (open circles) obtained by x-ray analysis in the TEM-AEM and calculated Ni profiles (lines) for several cooling rates. Hoba is a low Ni IVB and Warburton Range is a high Ni IVB iron.

A variation in the measured cooling rates of a factor of 6 or more for the IVB irons suggests that these irons cooled in a parent body whose mantle was not sufficiently thick to insulate the metallic core. Significant amounts of mantle could have been lost during catastrophic impact of the parent body before the temperature of the metallic core reached 1000 K. In addition, the size of the parent body should be much larger than the 3 km radius suggested by Rasmussen [4].

References: [1] Campbell A. J. and Humayun M. (2005) *Geochim. Cosmochim. Acta, 69,* 4733-4744. [2] Walker R. J. et al. (2008) *Geochim. Cosmochim. Acta, 72,* 2198-2216. [3] Rasmussen K. L. (1989) *Physica Scripta, 39,* 410-416. [4] Rasmussen et al. (1984) *Geochim. Cosmochim. Acta, 48,* 805-813. [5] Wood J. A. (1964) *Icarus, 3,* 429-459. [6] Goldstein J. I. and Ogilvie R. E. (1965) *Geochim. Cosmochim. Acta, 29,* 893-920. [7] Goldstein J. I. and Short J. M. (1967) *Geochim. Cosmochim. Acta, 31,* 1733-1770. [8] Yang J. et al. (2007) *Nature, 446,* 888-891. [9] Yang J. and Goldstein J. I. (2006) *Geochim. Cosmochim. Acta, 70,* 3197-3215. [10] Yang J. and Goldstein J. I. (2005) *Meteoritics & Planet. Sci., 40,* 239-253.